Catalyst−Nanostructure Interaction in the Growth of 1-D ZnO Nanostructures

C. Borchers,* S. Müller, D. Stichtenoth, D. Schwen, and C. Ronning

II. Physikalisches Institut, University of Göttingen, Göttingen, Germany

Received: August 10, 2005; In Final Form: November 17, 2005

Vapor−liquid−solid is a well-established process in catalyst guided growth of 1-D nanostructures, i.e., nanobelts and nanowires. The catalyst particle is generally believed to be in the liquid state during growth, and is the site for impinging molecules. The crystalline structure of the catalyst may not have any influence on the structure of the grown nanostructures. In this work, using Au guided growth of ZnO, we show that the interfaces between the catalyst droplet and the nanostructure grow in well-defined mutual crystallographic relationships. The nanostructure defines the crystallographic orientation of the solidifying Au droplet. Possible alloy, intermetallic, or eutectic phase formation during catalysis are elucidated with the help of a proposed ternary Au−Zn−O phase diagram.

Introduction

In the past few years, quasi-one-dimensional nanostructures have attracted considerable interest. A large variety of different materials have been fabricated as 1-D structures, including elemental and compound semiconductors,[1,2] borides, carbides, and carbonitrides,[3] metals,[4] polymers,[5−7] proteins,[8] water ice,[9] and even a ^{3}He quantum fluid.[10] Various techniques have been practiced in order to grow one-dimensional nanostructures. These include bottom-up techniques such as the vapor-solid (VS) process[11] and the vapor−liquid−solid (VLS) process[1,12,13] and top-down, i.e., lithographic techniques.[14] Furthermore there exist deposition techniques where the growth of nanostructures is supported by grated substrates,[15] or where they are embedded in matrixes.[4] Techniques where the material is confined into 1-D tubular structures[5−10] or the linear arrangement of granular material were also performed.[16,17]

Possible applications of 1-D nanostructures are diverse. Functional oxides and sulfides, with which this work is dealing, are fundamental ingredients of smart systems, because the physical and chemical properties can be tuned and controlled through adjusting cation valence and anion deficiency[2] as well as by ion implantation.[18] ZnO and ZnS exhibit properties covering almost all aspects of condensed matter physics including semiconductivity, superconductivity, ferroelectricity, magnetism, piezoelectricity, and chemical sensing.[2,19−21] VLS growth, one of the often applied methods to grow 1-D ZnO nanostructures, was already described in 1965 for gold-assisted growth of silicon whiskers,[1,12] and is well understood for this system. The metal liquid droplet serves as a preferential site for absorption of the vapor reactant. Nanostructure growth begins when the droplet is supersaturated with the source material and continues as long as the droplet is in the liquid state, and vapor is supplied. ZnO and ZnS 1-D nanostructures, among others, have been successfully grown by the VLS process despite the fact that the thermodynamics of the ternary system Au−Zn−O are poorly known. Since ZnO is known to decompose to a large extent at the evaporation temperatures used in this work,[22,23] the use of a pseudobinary phase diagram Au−ZnO is unsatisfactory.

It is the aim of this work to elucidate the thermodynamics of these systems. The considerations presented in this work will be purely deductive, supported on the knowledge of many known ternary phase diagrams[24−26] and own experience in the computation of binary phase diagrams.[27,28] The thermodynamic properties of the system Au−Zn−O can provide a deeper understanding of the properties any system requires for successful VLS growth. It may thus be helpful in choosing new material combinations for future applications. Furthermore, it will be shown that the Au catalyst droplet and the nanobelt or nanowire grown out of it exhibit distinct mutual orientation relationships once the droplet is solidified.

Experimental Section

The samples for this study were synthesized through a vapor−liquid−solid (VLS) process.[29] High-purity ZnO powders as source material were put in an alumina boat located at the center of a tube furnace, which was heated to 1350 °C. The source material temperature allows a substantial evaporation. Silicon substrates covered with a 15−20 nm thick Au film were placed at a position in the furnace where the temperature ranges between 960 and 1150 °C. The vapor was transported by Ar gas flow of 40 sccm to the substrates, at a pressure between 300 and 400 mbar.

X-ray diffraction data were collected with a Bruker AXS D8 Discover. Scanning electron microscopy (SEM) was performed with a LEO Supra 35 Gemini. Transmission electron microscopy (TEM) and high-resolution transmission electron microscopy (HRTEM) were performed on a Philips CM200 FEG UT at an acceleration voltage of 200 kV equipped with an energy-dispersive X-ray (EDX) detector. For SEM, the samples can be used in the as-prepared state, while for TEM, nanowires are posed onto copper grids covered with an amorphous carbon film by a wiping technique.

Results

In Figure 1a, a typical SEM micrograph of ZnO nanostructures can be seen. The structures are of ribbonlike shape, where the width is not constant for all structures. The tips of the ribbons are no more than about 100 nm broad. Most of these tips carry

* Present address: Institut für Materialphysik, University of Göttingen, Göttingen, Germany.

10.1021/jp054476m CCC: $33.50
Published on Web 01/06/2006

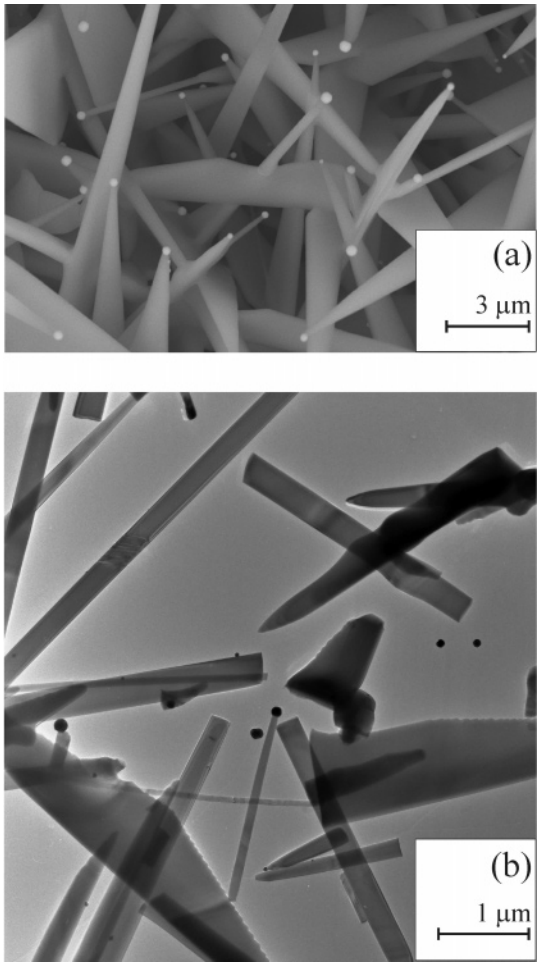

Figure 1. (a) SEM micrograph of ZnO nanostructures. The structures are triangular, where the tips of the triangles are no more than about 100 nm broad. Most of these tips carry a catalyst droplet. (b) TEM micrograph of such ZnO nanostructures, here exhibiting a rather belt-like shape. Here, too, catalyst droplets at the tips can be seen. Some catalyst droplets are detached from the ZnO belts and are lying loose on the TEM grid.

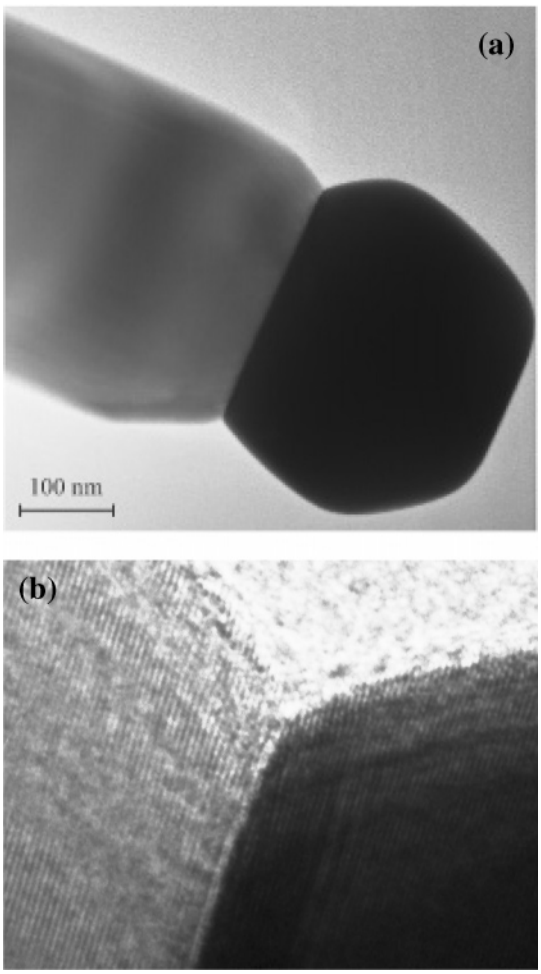

Figure 2. HRTEM micrograph of the interface between a ZnO nanostructure and its Au catalyst droplet, which appears dark. The lattice fringes of the two phases, ZnO and Au, are perfectly parallel to each other. The lattice spacing in the ZnO is 0.30 nm, corresponding to ZnO (0002). The lattice spacing in the Au droplet is 0.28 nm, corresponding to Au{110}. No evidence of a eutectic microstructure can be detected.

a catalyst droplet, which is white in the micrograph. Figure 1b shows a TEM micrograph of such ZnO nanostructures, here too exhibiting a belt-like shape. Catalyst droplets at the tips can be seen, dark in this micrograph. Some catalyst droplets are detached from the ZnO belts and are lying loose on the TEM grid.

Figure 2 shows a HRTEM micrograph of the interface between a ZnO nanostructure and its Au catalyst droplet, which appears dark. Figure 2a is an overview, while Figure 2b is a close-up of the interface. The lattice fringes of the two phases, ZnO and Au, are perfectly parallel to each other. The lattice spacing in the ZnO is 0.30 ± 0.03 nm, corresponding to ZnO (0002). The lattice spacing in the Au droplet is 0.28 ± 0.03 nm, corresponding to the forbidden Au {110}. No evidence of a eutectic microstructure can be detected. In XRD investigations, the ZnO (0002) lattice spacing was established as 0.26 ± 0.01 nm.

Discussion

The VLS growth mechanism is fully understood for the binary system Au−Si.[1,12] When Si atoms impinge on Au droplets, a liquid Au−Si solution is formed. The surface of the liquid has a large accommodation coefficient and is the preferred site for deposition. The liquid solution receives a flux of material from its surface. The resulting concentration gradient provides the driving force for diffusion from the surface to the inside of the droplet and to the substrate−liquid interface. The liquid becomes supersaturated with material supplied from the vapor and crystal growth occurs by heterogeneous precipitation at the substrate−liquid interface. There are major requirements for successful VLS growth: there must be a eutectic in the respective alloy system, and the mutual solubility in the solid state must be very small, as is the case for the system Au−Si. Up to date, a multitude of binary and even ternary 1-D nanostructural semiconductors have been grown by the VLS mechanism.[13,30] It has been assumed that the catalyst−semiconductor systems can be treated as pseudobinary systems.[31] In this framework, it is assumed that the catalyst and the compound semiconductor are immiscible in the solid state. For the combination ZnS/Au, which from a chemical point of view resembles the ZnO/Au, this assumption finds support from geological findings: In studies of Au−Zn mineralization, ZnS was found as sphalerite (cubic ZnS), and Au as pure metal. Sphalerite crystals were checked for solutes: Fe, Cd, Sb, and Cu were found, but no Au.[32] However, studies of ZnO vaporization[22,23] showed that mass spectrometric intensities of ZnO in the vapor are about 3 orders of magnitude lower than the intensities of Zn and O_2 in a temperature range that includes the evaporation temperature of 1350° used for nanowire growth. This result makes the use

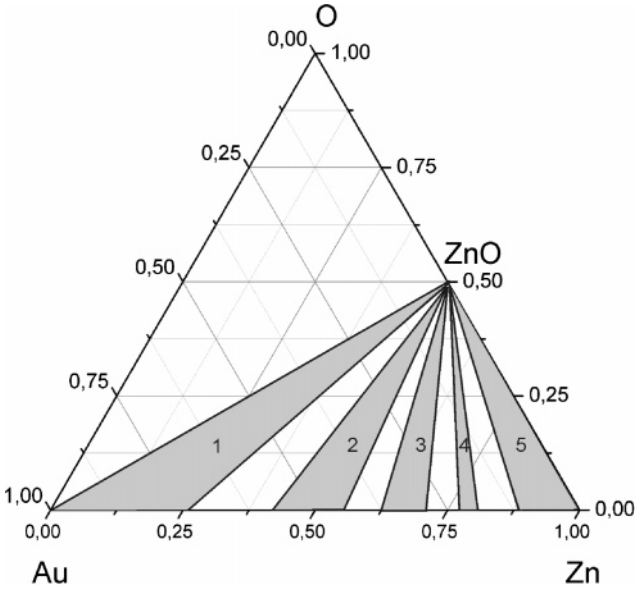

Figure 3. Tentative ternary Au−Zn−O phase diagram, an isothermal section at about 550 °C is sketched. Two-phase regions are gray: (1) (Au) + ZnO, (2) AuZn + ZnO, (3) $AuZn_3$ + ZnO, $AuZn_4$ + ZnO, and (5) L + ZnO, where L is the Zn-rich liquidus. The white regions are three-phase regions.

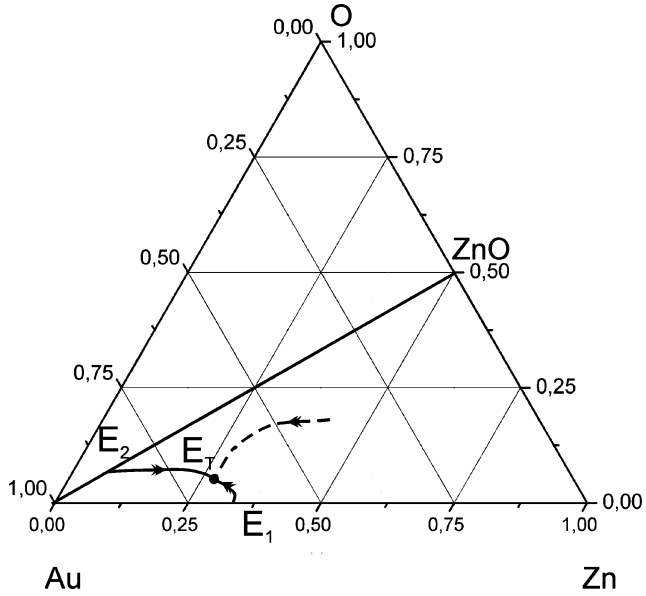

Figure 4. Tentative liquidus surface of the proposed phase diagram. E_1: eutectic L ↔ (Au) + AuZn at 683 °C and 33.5 at.% Zn. E_2: quasibinary eutectic between Au and ZnO: L ⇌ (Au) + ZnO at 650 °C < T < 1000 °C. E_T: ternary eutectic L ⇌ (Au) + ZnO + AuZn at $T \leq 650$ °C.

of a pseudobinary phase diagram for Au−ZnO unsatisfactory, as soon as the vapor phase is involved.

To our knowledge, the ternary phase diagram of the Au−Zn−O system is not known. A tentative ternary phase diagram is therefore proposed in this work. A look at the three binary diagrams shows that the O miscibility in Au is smaller than 10^{-4} in the liquidus as well as in the solid state. There is a high-pressure intermediate crystalline phase Au_2O_3 that decomposes under ambient pressure at about 175 °C.[33,35] The exact Au−O phase diagram is not known either, but general considerations lead to the assumption that there is an equilibrium of unknown type in which the liquid and solid Au-rich solutions are involved, at a concentration very near pure Au and a temperature near the melting temperature 1064 °C of pure Au. The situation is similar for the Zn−O system: we assume a ternary reaction L + (Zn) + ZnO near the melting temperature 420 °C of pure Zn at a concentration very near pure Zn,[33] and another ternary rection at a concentration near pure ZnO. There is a miscibility gap in the liquidus. The melting temperature of ZnO is 1972 °C,[33] but, as stated above, there is evidence that it rather decomposes into Zn and O_2.[22,23] The phase diagram of Au−Zn is in contrast well-known.[33] There are numerous intermetallic phases, and two eutectic points, of which the one on the Au-rich side is of interest here: L ↔ (Au) + AuZn at 683 °C and 33.5 at % Zn. AuZn has a congruent melting point at 753 °C. To our knowledge, no ternary solid phase has been reported for Au−Zn−O. This is confirmed by the fact that the JCPDS database provided by the international center for diffraction data does not list any ternary phases for this combination.[34]

We now propose a ternary Au−Zn−O phase diagram, an isothermal section at about 550 °C, which is sketched in Figure 3. We are starting from the assumption that ZnO and the solid Au−Zn intermetallic phases are virtually immiscible in the solid state, just as the pure substances Au and Zn are virtually immiscible with ZnO. The quasibinary system Au−ZnO divides the whole system into two parts: Au−ZnO−O and Au−Zn−ZnO. Similar ternary phase diagrams are known for the ternary alloys Al−Mg−Si[26,36] and Al−Ca−Si.[26,37]

Since VLS growth is known to happen on the Zn-rich side,[29] the partial system Au−ZnO−O will not be considered any further. Two-phase regions are gray and marked with numbers: (1) (Au) + ZnO, (2) AuZn + ZnO, (3) $AuZn_3$ + ZnO, (4) $AuZn_4$ + ZnO, and (5) L + ZnO, where L is the Zn-rich liquidus as described above. The extensions of the two-phase regions can be derived from the binary Au−Zn diagram.[33] The white regions are three-phase regions. Of special interest for Au-assisted VLS growth of ZnO is the three-phase region between 1 and 2 in Figure 3, namely (Au) + ZnO + AuZn. From the binary eutectic point at 33.5 at % Zn, a ternary melting path must lead to a ternary eutectic equilibrium: L ⇌ (Au) + ZnO + AuZn at $T \leq 650$ °C. Another melting path must lead to this eutectic point from a quasibinary eutectic between Au and ZnO: L ⇌ (Au) + ZnO at 650 °C < T < 1000 °C. In Figure 4, a liquidus surface of the Au−Zn−O system is proposed, illustrating the above considerations. A tentative isothermal section at 1100 °C of the proposed phase diagram is shown in Figure 5. Since Zn is immiscible with ZnO in the liquid state,[33] there is a ternary liquidus miscibility gap.[26] Upon Au depletion, the Au-rich liquidus L branches into ZnO-rich L′ and Zn-rich L″. Near ZnO, there is a two-phase field ZnO + L′, and between ZnO and Zn, there is a three-phase field ZnO + L′ + L″. Although there can be no doubt that an unmixing can be found in the melt, the location of the critical point of the Au-rich liquidus in the phase diagram is purely hypothetical, the same applies to the solidus between ZnO and L′.

When during the VLS process Zn and O_2, and to a lesser extent ZnO, impinge on the Au particle, the particle melts and takes up Zn and O_2. The composition of the liquid alloy proceeds from pure Au toward ZnO into the L′ branch of the liquidus. Eventually L′ supersaturates, and ZnO is precipitated in solid form from the melt. This can take place as long as the temperature is held and as long as the supply of Zn and O_2 is guaranteed. Upon cooling, the liquidus turns Au-rich. The Au droplet solidifies. Since this is not yet the minimum liquidus temperature, some material can remain molten upon further cooling, if excess Zn is available. At this stage, the melt cannot

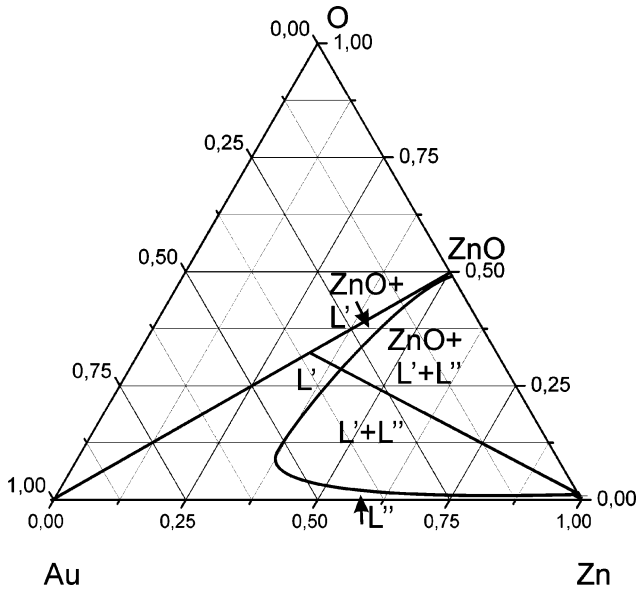

Figure 5. Tentative isothermal section at 1100 °C of the proposed phase diagram.

take up any O. During the cooling, Zn is still in the atmosphere of the furnace. So the ternary eutectic E_T can be reached at some temperature below 650 °C, where, if equilibrium is given, the melt must solidify to (Au), ZnO, and AuZn, see Figure 4. It is known, though, that ternary eutectics are often degenerate, i.e., only two of the three phases crystallize.[26] A reason for this could be that one of the phases has difficulties in crystallizing because its structure is incompatible with the others or complicated, as is the case for the ternary eutectic in the system Al−Ni−Cu.[26] In the case discussed here, it could be the intermetallic AuZn that does not appear. The final solidification will most probably take place in the inside of the droplet, since the temperature falls from the outside to the inside, and consequently solid precipitation happens at the outside first. Because of the size of several 100 nm of the catalyst droplets, it is not possible to elucidate details of the droplet's nanostructure by TEM. EDX measurements did not yield substantial Zn contents in the droplets, so they do not contradict the notion of a droplet with a rather thick shell of Au-rich solid solution and a core composed of three phases, (Au), ZnO, and perhaps AuZn, solidified out of a eutectic melt.

There is a striking observation in our results: The lattice spacing in the (ZnO)-Au droplet is 0.285 nm, corresponding to Au {110}. Au {110} is a forbidden reflection, it can only be seen in fcc-based superstructures such as $L1_2$ (prototype Cu_3-Au). The question arises, whether Au could have formed an alloy with ZnO, Zn, or O. According to the ternary phase diagram proposed in this work, only Au/Zn intermetallic phases exist, namely, Au_3Zn, AuZn, $AuZn_2$, and $AuZn_3$, some of which adopt several crystal structures.[33] Yasuda and Mori deposited Zn on Au clusters about 6.5 nm in mean diameter.[38] They observed spontaneous formation of compound clusters: Au_3-Zn and AuZn.[38] Now Au_3Zn adopts a tetragonally distorted $L1_2$ structure with lattice constants $a = 0.402$ nm and $c = 0.410$ nm. The tetragonal distortion is due to a long-period anti-phase structure of Au_3Zn.[39] AuZn adopts a B2 CsCl-type structure with $a = 0.319$ nm.[38] The latter structure has no main lattice spacing of 0.285 nm, but the Au_3Zn {110} lattice spacing coincides with that of Au {110}, since $L1_2$ is a superstructure of the fcc lattice.

We assume that a thin layer of Au_3Zn might have formed on the surface of the already solidified Au droplet during cooling,

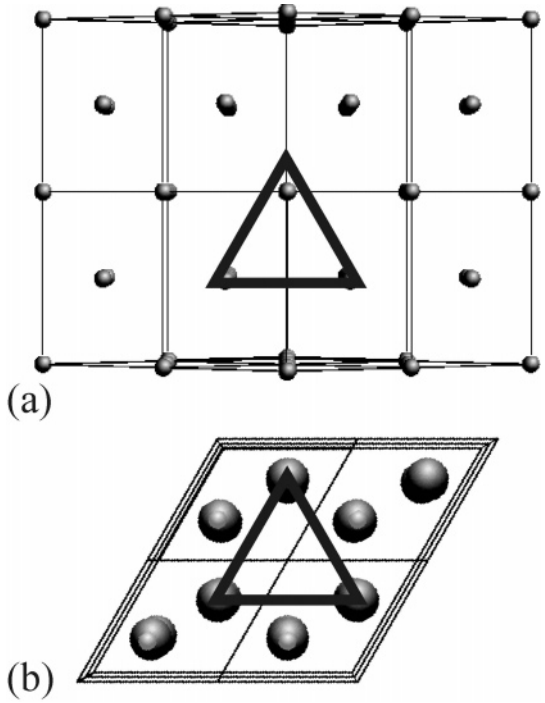

Figure 6. Orientation relationship of the ZnO−Au droplet interface. Top: Au⟨110⟩. Bottom: ZnO⟨0002⟩. Taken from EMS OnLine.[40] A triangle demonstrates the orientation relationship.

when Zn vapor is still available. Any available O_2 will not be taken up by the solid droplet. A surface layer of 5 nm thickness on a droplet with a radius of 100 nm would be equivalent to an overall Zn concentration of about 3% in the droplet, which is a quantity that fits well with our EDX results.

From the fact that the lattice fringes in Figure 2 are perfectly parallel, one can deduce that the corresponding lattice planes are arranged in an epitactical relationship. The terminating ZnO plane is (0002). Things are not so clear in the case of Au. The Au droplet exhibits {110} fringes, most probably of Au_3Zn. When these planes are coherent to each other, $\langle 10\bar{1}0\rangle_{Zn}||\langle 110\rangle_{Au}$ with a misfit of 2.2%,[40] and $\langle 01\bar{1}0\rangle_{Zn}||\langle 002\rangle_{Au}$ with a misfit of 16.5%. These misfits are of the same order of magnitude as in the well-known Nishiyama−Wassermann-relationship, where $\langle 110\rangle_{bcc}||\langle 111\rangle_{fcc}$.[40,41] The coherency relationship of the ZnO/Au interface is sketched in Figure 6, where part a shows a projection of a Au {110} plane, and part b shows a projection of a ZnO (0002) plane. A triangle demonstrates the orientation relationship. The diagrams are taken from EMS OnLine.[42]

In Figure 1b, catalyst droplets, lying loose on the TEM grid, can be seen. This observation can be explained by energetic considerations: in coherent growth, the coherent strain energy γ_{coh} can be estimated as follows:

$$\gamma_{coh} = 2\frac{1+\nu}{1-\nu}\mu\epsilon^2 d \qquad (1)$$

with ν being the Poisson ratio, $\mu = 4.23 \times 10^{10}$ J/m^3 being the shear modulus of Au, ϵ being the coherent misfit, and d being the mean distance between misfit dislocations, which should be some nm. This coherent strain energy can now be estimated to be on the order of some J/m^2. Surface energies are of the same order, which makes the formation of new surfaces easy from the point of view of energetics, so solid droplets can easily detach from the wire during sample preparation for TEM, which is a technique involving mechanical manipulation of the samples.

Conclusions

A ternary phase diagram to help understand the Au-assisted vapor−liquid−solid growth of ZnO nanobelts and nanowires is proposed in this work. As in the systems Al−Mg−Si and Al−Ca−Si, a quasibinary subsytem, here Au−ZnO governs the thermodynamic appearance of the phase diagram. Because ZnO is known to be dissociated to a large extent upon vaporization, the quasibinary subsystem alone is not sufficient to describe the growth behavior. It is deduced that upon cooling, a ternary eutectic governs the solidification of the Au catalyst droplet. Further work will have to be done to substantiate our considerations concerning the ternary phase diagram Au−Zn−O.

Acknowledgment. This work was supported by the Deutsche Forschungsgemeinschaft via the main focus program "Nanowires and Nanotubes", grant no. Ro 1198/7-1, which is gratefully acknowledged.

References and Notes

(1) Wagner, R. S.; Ellis, W. C. *Appl. Phys. Lett.* **1964**, *4*, 89.
(2) Wang, Z. L. *Annu. Rev. Phys. Chem.* **2004**, *55*, 159.
(3) Johnson, M. *Solid State Ionics* **2004**, *172*, 365.
(4) Sauer, G.; Brehm, G.; Schneider, S.; Graener, H.; Seiffert, G.; Nielsch, K.; Choi, J.; Göring, P.; Gösele, U.; Miclea, P.; Wehrspohn, R. B. *J. Appl. Phys.* **2005**, *97*, 024308.
(5) Yang, P.; Chowdhury, A.; Holman, M. W.; Adams, D. M. *J. Phys. Chem. B* **2005**, *109*, 724.
(6) Hasegawa, T.; Haraguchi, S.; Numata, M.; Fujisawa, T.; Li, C.; Kaneko, K.; Sakurai, K.; Shinkai, S. *Chem. Lett.* **2005**, *34*, 407.
(7) Tai, X.; Wu, G.; Tominaga, Y.; Asai, S.; Sumita, M. *J. Polym. Sci.* **2005**, *43*, 184.
(8) Yui, H.; Shimizu, Y.; Kamiya, S.; Yamashita, I.; Masuda, M.; Ito, K.; Shimizu, T. *Chem. Lett.* **2005**, *34*, 232.
(9) Fois, E.; Gamba, A.; Tabacchi, G.; Quartieri, S.; Vezzalini, G. *Phys. Chem. Chem. Phys.* **2001**, *3*, 4158.
(10) Taniguchi, J.; Yamaguchi, A.; Ishimoto, H.; Ikegami, H.; Matsushita, T.; Wada, N.; Gatica, S. M.; Cole, M. W.; Ancilotto, F.; Inagaki, S.; Fukushima, Y. *Phys. Rev. Lett.* **2005**, *94*, 065301.
(11) Wang, Z. L.; Kang, Z. C. *Functional and Smart Materials*; Plenum: New York, 1998.
(12) Wagner, R. S.; Ellis, W. C. *Trans. Metall. Soc. AIME* **1965**, *233*, 1053.
(13) Law, M.; Goldberger, J.; Yang, P. *Annu. Rev. Mater. Res.* **2004**, *34*, 83.
(14) Gates, B. D.; Xu, Q.; Love, J. C.; Wolfe, D. B.; Whitesides, G. M. *Annu. Rev. Mater. Res.* **2004**, *34*, 339.
(15) Herweg, C. Thesis, University of Göttingen, 2005.
(16) Snezhko, A.; Aranson, I. S.; Kwok, W. K. *Phys. Rev. Lett.* **2005**, *94*, 108002.
(17) Gui, Z.; Liu, J.; Wang, Z.; Song, L.; Hu, Y.; Fang, W.; Chen, D. *J. Phys. Chem. B* **2005**, *109*, 1113.
(18) Ronning, C.; Gao, P. X.; Ding, Y.; Wang, Z. L.; Schwen, D. *Appl. Phys. Lett.* **2004**, *84*, 783.
(19) Huang, Y.; Lieber, C. M. *Pure Appl. Chem.* **2004**, *76*, 2051.
(20) Li, C.; Zhang, D.; Han, S.; Liu, X.; Tang, T.; Lei, B.; Zhou, C. *Ann. N.Y. Acad. Sci.* **2003**, *1006*, 104.
(21) Kolmakov, A.; Moskovits, M. *Annu. Rev. Mater. Res.* **2004**, *34*, 151.
(22) Grade, M.; Hirschwald, W.; Stolze, F. *Z. Phys. Chem. Neue Folge* **1976**, *100*, 165.
(23) Makarov, A. V.; Zbezhneva, S. G.; Kovalenko, V. V.; Rumyantseva, M. N. *Inorg. Mater.* **2003**, *39*, 594.
(24) *Ternary alloys*: *a comprehensive compendium of evaluated constitutional data and phase diagrams*; Petzow, G., Effenberg, G., Eds.; VCH: Weinheim, Germany, 1988−1998.
(25) *Ternary alloys*: *a comprehensive compendium of evaluated constitutional data and phase diagrams*; Effenberg, G., Ed.; MSI: Stuttgart, Germany, 1999−.
(26) Hanemann, H.; Schrader, A. *Ternäre Legierungen des Aluminiums*, *Atlas Metallographicus*, *III.2*; Verlag Stahleisen mbH: Düsseldorf, Germany, 1952, in German.
(27) Borchers, C. Thesis, University of Göttingen, 1992.
(28) Borchers, C.; Bormann, R. *Acta Mater.* **2005**, *53*, 3695.
(29) Wang, Z. L. *Nanowires and Nanobelts Materials*, *Properties and Devices Metal and Semiconductor Nanowires*; Kluwer: Dordrecht, The Netherlands, 2003; Vol. I.
(30) Jie, J.; Wang, G.; Han, X.; Fang, J.; Yu, Q.; Liao, Y.; Xu, B.; Wang, Q.; Hou, J. G. *J. Phys. Chem. B* **2004**, *108*, 8249.
(31) Duan, X.; Lieber, C. M. *Adv. Mater.* **2000**, *12*, 298.
(32) Palacios, C.; Parada, M. A.; Lahsen, A. *Geol. Rundsch.* **1997**, *86*, 132.
(33) Okamoto, H.; Massalski, T. B. In *Binary Alloy Phase Diagrams*; Massalski, T. B., Okamoto, H., Subramanian, P. R., Kacprzak, L., Eds.; ASM International: Materials Park, OH, 1990.
(34) Knacke, O.; Kubaschewski, O.; Hasselmann, K. *Thermochemical Properties of Anorganic Substances*; Springer: Berlin, Germany, 1991.
(35) http://www.icdd.com.
(36) Chakraborti, N.; Lukas, H. L.; Bodak, O.; Rokhlin, L. In *Ternary alloys*; Effenberg, G., Ed.; MSI: Stuttgart, Germany, 1999; Vol. 16, p 382.
(37) Schmidt-Fetzer, R. In *Ternary alloys*; Petzow, G., Effenberg, G., Eds.; VCH: Weinheim, Germany, 1990; Vol. 3, p 628.
(38) Yasuda, H.; Mori, H. *Phys. Rev. Lett.* **1992**, *69*, 3747.
(39) Laihia, R.; Kokko, K.; Leiro, J. A.; Mansikka, K. *J. Phys.*: *Condens. Matter* **1995**, *7*, 5521.
(40) Nishiyama, Z. *Sci. Rep. Tohoku Univ.* **1934**, *23*, 638.
(41) Wassermann, G. *Arch. Eisenhuettenwes.* **1933**, *16*, 647.
(42) Jouneau, P. H.; Stadelmann, P. *EMS OnLine* **2005**, http://cimesgt1.epfl.ch/CIOL/ems.html.